

# Ligand-tagged cationic liposome facilitates efficient gene delivery to folate receptors

Sridevi Gorle\*, Alisha Sewbalas, Mario Ariatti and Moganavelli Singh

Non-viral Gene Delivery Laboratory, Discipline of Biochemistry, University of KwaZulu-Natal, Chiltern Hills, Durban-4000, South Africa

**Non-viral cationic liposome/DNA complexes (lipoplexes) have been used extensively in gene delivery approaches, although they have shown lower efficiency compared to viral carriers. In this study, a rational strategy was employed taking advantage of a combination of cationic liposomes prepared using the cationic cytofectin MSO9 and a folate ligand to create a more selective and effective gene delivery system to target cancer cells that overexpress the folate receptor (FR). The folate receptor-negative HEK293 (FR-), and folate receptor-positive HeLa (FR+) and KB (FR++) cell lines were employed to evaluate the efficiency of this novel gene delivery system under serum conditions. Folate was conjugated to the distal ends of DSPE-PEG<sub>2000</sub> to create DSPE-PEG<sub>2000</sub>-FOL, which was then incorporated into the cationic liposomal bilayer. Our observations indicate that FA-labelled lipoplexes confer greater DNA protection, with PEGylated systems (liposome:pDNA) producing smaller-sized particles (<200 nm) ensuring appropriate pDNA release and targeted delivery. Moreover, FA-labelled lipoplexes attained higher transfection activity over nonfolate-labelled lipoplexes in FR-positive cell lines as confirmed by the luciferase and flow cytometry assays. Our results collectively highlight the potential of this lipid-based targeted gene delivery approach for future *in vivo* applications.**

**Keywords:** Cationic liposome, folate receptor, gene delivery, transfection.

ALTHOUGH the nucleus is the target organelle for gene delivery protocols in mammalian cells, the nucleic acid cargo must first be introduced into the cytoplasm of the desired cell population in a targeted and integral manner<sup>1</sup>. Compared to viral vectors, non-viral gene delivery vectors allow safe delivery of genetic material with less inherent immunogenicity and oncogenicity. The goal of non-viral gene delivery is to correct a gene defect by intracellular delivery of nucleic acids. Non-viral vectors for gene delivery usually comprise formulations of cationic polymers or liposomes that self-assemble electrostatically upon mixing with nucleic acids at optimized ratios to form cationic nanocomplexes that are often effective as *in vitro* transfection agents. However, they also display poor

transfection efficiency *in vivo* due to their aggregation in serum and non-specific, charge-mediated binding to anionic cell surfaces and extracellular adhesion molecules<sup>2</sup>. Gene delivery using synthetic, non-viral elements continues to motivate research efforts since the first report by Felgner *et al.*<sup>3</sup> on the use of the cationic lipid *N*-[1-(2,3-dioleoyloxy) propyl]-*N,N,N*-trimethylammonium (DOTMA) as a vehicle for nucleic acid delivery. Synthetic lipids, due to their low toxicity, relative ease of large-scale production and purification, coupled with their ability to exist in many self-assembled macromolecular shapes under varying conditions of formulation provide a versatile material for lipofection. Majority of synthetic non-viral lipids for transfection contain a positively charged head group, typically tertiary or quaternary ammonium groups or polyamines, and a hydrophobic domain based on either alkyl chains or cholesterol and a spacer<sup>4</sup>. Excessive positive charges on vectors can ultimately undermine the transfection efficiency. Therefore, it is of particular importance to balance the charge-related membrane activity and cytotoxicity in the design of non-viral vectors such that the gene delivery efficiency could be maximized<sup>5</sup>. Protection (from serum nucleases) and cellular delivery of the genetic cargo are achieved by packaging the integrally negatively charged nucleic acid with the cationic liposomes into a compacted particle (a lipoplex), driven by electrostatic and hydrophobic interactions<sup>6,7</sup>. The success of the gene transfer vectors, characterized by a heterocyclic polar head group, has been attributed in large measure to the delocalized positive charge which offers a favourable electrostatic interaction<sup>8</sup>. This diffuse charge offers precisely an appropriate balance between binding the nucleic acid cargo and subsequent cargo release through endosomal escape<sup>8</sup>. Strategies to improve the efficiency and biocompatibility of cationic elements for gene delivery typically involve grafting the functional ligands, such as lipids, peptides and sugars or a combination thereof, to advance the stability, targeting, uptake and sub-cellular trafficking capabilities of the carrier<sup>9</sup>.

The last few decades have witnessed ligand-modified nano-carriers being extensively studied in probing for a more specific targeting strategy for their potential clinical use in cancer therapy<sup>10,11</sup>. Targeted delivery has therefore attracted much attention in anticancer research due to advantages such as enhanced distribution in tumour sites

\*For correspondence. (e-mail: srideviskt@gmail.com)

and reduced side effects in normal tissues<sup>12</sup>. Targeted/site-specific gene delivery commonly refers to a category of therapeutic systems that are able to accumulate only at diseased sites. Historically, this site-specific targeting delivery can be divided into two types: 'passive' and 'active'. The former is primarily due to the enhanced permeability and retention (EPR) effect. Tumours generally grow fast, leading to highly heterogeneous and aberrant forms. As a result, particles in a suitable size range readily extravasate from surrounding vessels into the tumour site. Active targeting improves the efficacy further by surface modification of the nanoparticles (NPs) with a targeting ligand. The ligand assists the NPs in penetrating into cancer cells which are characterized by overexpression of the corresponding receptor<sup>13</sup>. The introduction of various biological ligands or antibodies into delivery systems can provide the opportunity for selective delivery to tumour cells. Such ligands are recognized by specific receptors on cancer cell surfaces, which may induce cellular uptake of the ligand-tagged vectors via the receptor-mediated endocytosis mechanism. Among cancer cell-specific ligands, folate, a small-molecule-targeting ligand, has been conjugated to a wide variety of carriers, and has demonstrated extremely successful delivery to several folate receptor-positive (FR+) tumour cells both *in vitro* and *in vivo*. This has been promoted by its low cost, small size, convenient modification, commercial availability, specificity and high binding affinity ( $K_d \sim 10^{-10}$  M) for FR. Also, FR is a 38 kDa glycosyl phosphatidylinositol-anchored protein overexpressed in many primary and metastatic cancers, including ovarian and breast cancers, while its expression is highly restricted in normal cells<sup>14</sup>. Besides the above advantages of folate, its poor water solubility was reported to display lower exposure and accessibility to FRs. However, an increase in the folate content may perhaps lead to saturation of folate concentration and could increase the amount of folate present on the surface. Consequently, this may also diminish the water solubility of the carrier/vector, thereby negatively influencing the release profile of the therapeutics and an undesirable increase in the phagocytosis by macrophages in the circulation. Conversely, we hypothesized that upon cell-membrane adhesion, which brings the conjugate in close proximity to the cell surface, the chance for folate to interact with FR might also increase, leading to a synergic enhancing effect on cellular uptake by both ligand receptor interaction and electronic attraction<sup>11</sup>. In a study by Valencia *et al.*<sup>15</sup> only 20% of the folate from PLGA-PEG-folate was present on the NP surface, while the rest remained presumably buried in the PLGA NP core due to hydrophobic interactions of PLGA and folate. Furthermore, the attached therapeutic cargo must be membrane-permeable, since FR+ endosomes contain no pores or channels through which hydrophilic or polymeric drugs can diffuse. Nevertheless, because these limitations are easily

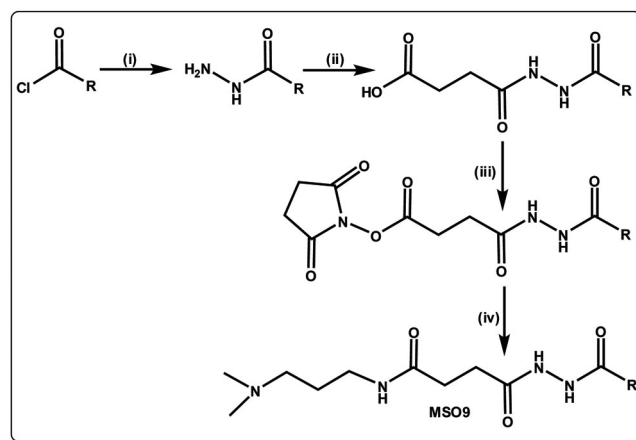
surmountable for many cancers and their preferred therapeutic agents, the prospects for clinical success of a folate-targeted delivery system seem promising<sup>16</sup>. Folic acid retains its receptor-binding and endocytic properties when covalently linked to a variety of molecules.

Therefore, liposomes conjugated to a folate ligand via a PEG-spacer have been used for the delivery of chemotherapeutic agents and DNA to receptor-bearing tumour cells, e.g. a human nasopharyngeal cancer cell line, KB<sup>17</sup>.

## Results and discussion

### *Synthesis of N,N-dimethylpropylamidossuccinylcholesterylesterlylformylhydrazide (MSO9)*

The synthesis of cationic cytofectin MSO9 has been reported earlier<sup>18</sup> and is outlined in Scheme 1. Briefly, the first step afforded cholesterylformylhydrazide (MSO4) by the reaction of cholesteryl chloroformate with hydrazine ( $N_2H_4$ ; electron donor). This may be described as a dehydrohalogenation reaction. In the second step, the cholesterylformylhydrazide amino group was treated with succinic anhydride ( $C_4H_4O_3$ ) in the presence of a dimethylformamide:pyridine solvent system (1/1 v/v) to yield the intermediate compound cholesterylformylhydrazide hemisuccinate (MSO8). The MSO8 synthesis results in the expansion of the spacer segment by succinylation. The third step is the preparation of *N*-hydroxysuccinimide ester of cholesterylformylhydrazide hemisuccinate (NHS ester of MSO8) by reacting MSO8 with equimolar ratios of DCC : NHS (1 : 1), in preparation for the addition of a cationic head group. The MSO8 carboxyl group was first activated by DCC, followed by reaction with NHS to generate the reactive ester of MSO8. In the final step, the amine group of dimethylaminopropylamine (DMAPA) was coupled to the carboxyl group on the NHS ester of



**Scheme 1.** Synthesis of MSO9. Reagents and conditions: (i) Hydrazine in  $CHCl_3/MeOH$ ; (ii) succinic anhydride in pyridine/DMF; (iii) DCC/NHS in DMF and (iv) dimethylaminopropylamine in  $H_2O$ /pyridine/DMF.

MS08 via an amido link to afford the final compound, MS09.

### Morphology of liposomes and lipoplexes

Cryo-TEM provides direct visualization of liposome assembly, quantitative measurements of various size metrics, physical properties and definitive characterization of encapsulated gene/drug<sup>19</sup>. The preparations predominantly showed unilamellar vesicles with a narrow size distribution, as seen in particle size analysis. Liposomes were generally spherical or elliptical in shape (Figure 1 *a–c*). The morphology of liposomes was altered upon complexation with pDNA (Figure 1 *d–f*), with singular globular shapes being replaced by cluster formations. Furthermore, no visible agglomeration of preparations was visible.

### Liposome–nucleic acid interactions

*Gel retardation assay:* pDNA binding affinity must be considered as an important parameter in the formation of liposome–pDNA complexes. Herein, pDNA binding affinities of MS09 liposomes were evaluated by agarose gel retardation assay. The migration pattern of pCMV-luc DNA changed when the pDNA was complexed to the liposome particles at charge ratios from 1:1 to 7:1. Electrophoretic images show that the intensity of free

pDNA migrating bands gradually decreased as the charge ratios increased (Figure 2). Furthermore, the pCMV-luc DNA was completely retarded upon the addition of lipoplexes at a  $\pm$  ratio of 3 for both unPEGylated and PEGylated, targeted liposomes. No migration of pDNA was observed beyond this point as all the DNA was liposome-bound and remained in the wells. Cationic head group-bearing lipids possessed higher pDNA binding affinities, which could be attributed to the combination effect of the electrostatic and hydrophobic interactions<sup>20,21</sup>. PEGylated lipoplexes showed lower binding affinities compared to the unPEGylated, targeted lipoplexes. As shown in Figure 2, PEGylated liposomes could completely bind the pDNA at a charge ratio 2:1. Modification of cationic liposomes with PEG extends the circulation lifetime of the cationic liposomes. However, PEGylation often results

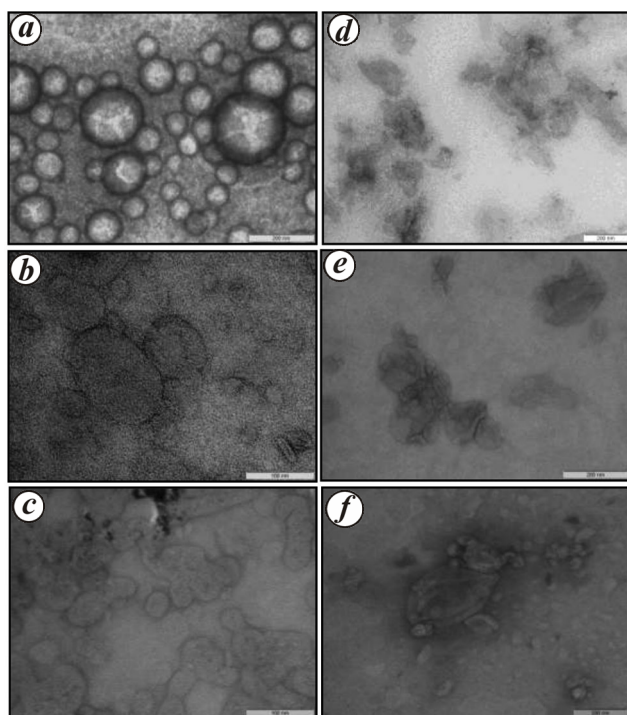


**Figure 1.** Transmission electron microscopic images of MS09 non-targeted, PEGylated and targeted liposomes (*a–c*) and their respective lipoplexes (*d–f*). Bar = 200 nm.

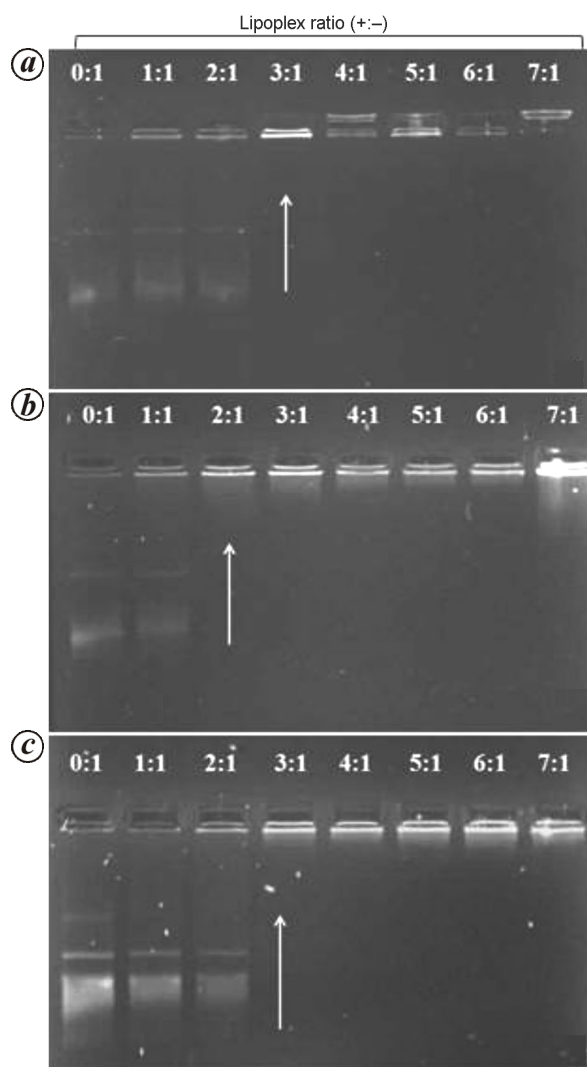


**Figure 2.** DNA-binding studies of MS09 liposomes using 0.5 µg of pCMV-luc DNA. One per cent agarose gel electrophoresis of complexes at indicated  $\pm$  charge ratios from 1:1 to 7:1 (lanes 2–8). *a*, Non-targeted lipoplexes, *b*, PEGylated lipoplexes and *c*, Targeted lipoplexes in HBS (10 µl) along with control (lane 1).

**Table 1.** Liposome composition, size and zeta potential analysis of MSO9 particles

Formulation	Liposome										
	Composition ( $\mu\text{mol}/0.5\text{ ml}$ )						Lipoplex				
	MSO9	DOPE	DSPE- PEG <sub>2000</sub>	DSPE- PEGFOL	Size <sup>b</sup> (nm)	PDI	Zeta potential <sup>b</sup> (mV)	Charge ratio ( $\pm$ ) <sup>a</sup>	Size <sup>b</sup> (nm)	PDI	Zeta potential <sup>b</sup> (mV)
MSO9 : DOPE	1	1	–	–	196 $\pm$ 2.17	0.22	24.07 $\pm$ 9.69	3 : 1	695 $\pm$ 112.56	0.57	8.07 $\pm$ 1.24
MSO9 : DOPE : 2%PEG <sub>2000</sub>	1	0.96	0.04	–	121 $\pm$ 1.62	0.23	22.23 $\pm$ 0.81	2 : 1	106 $\pm$ 0.46	0.21	–3.37 $\pm$ 0.15
MSO9 : DOPE : 2%PEG <sub>2000</sub> : DSPE-PEGFOL	1	0.96	0.04	0.01	168 $\pm$ 2.91	0.33	19.33 $\pm$ 0.40	3 : 1	191 $\pm$ 11.63	0.47	–14.31 $\pm$ 2.71

<sup>a</sup>Charge ratios were calculated assuming that MSO9 carries a positive charge at physiological pH and that the average molecular weight of pDNA nucleotides is 330 Da, with each carrying one negative charge. <sup>b</sup>The results are given as the mean  $\pm$  SD ( $n = 3$ ).

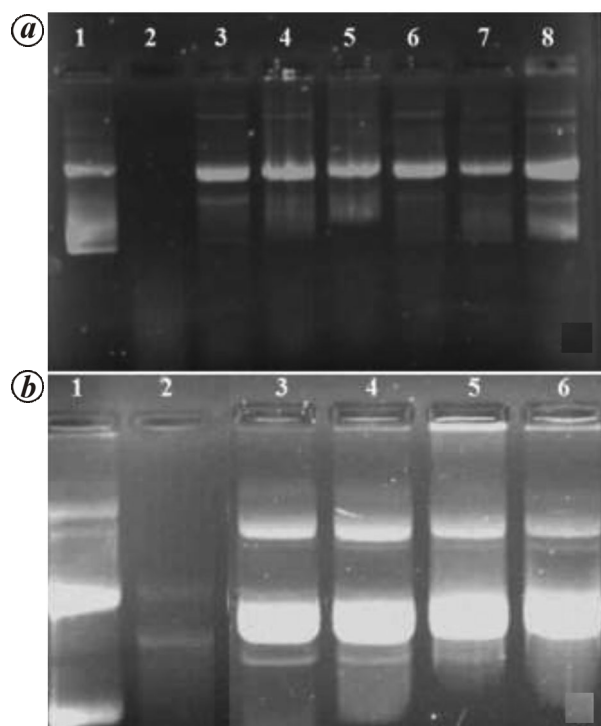


**Figure 3.** Nuclease digestion assays of MSO9 lipoplexes. Complexes below, above and optimal end-point gel retardation  $\pm$  ratios were tested for DNA-protection studies (lane 1). Untreated pDNA (lane 2). Treated pDNA. *a*, Non-targeted lipoplexes (lanes 3–5) and targeted lipoplexes (lanes 6–8) at 2 : 1–4 : 1 ratios. *b*, PEGylated lipoplexes (lanes 3–6) at 1 : 1–3 : 1 ratios. pDNA was constant at 0.5  $\mu\text{g}$  in all the lanes.

in low gene entrapment efficiency due to the decline of positive surface charge<sup>22</sup>.

**Nuclease digestion assay:** This assay was used to determine the accessibility of liposome-associated pDNA to nucleases present in the serum. Essentially, all lipoplex formulations assayed offered a moderate-to-high degree of pDNA protection based on their formulation against nuclease degradation. Liposome formulations employing a 2 mol% PEG (PEGylated) afforded greater protection (Figure 3 *a*) to the DNA cargo than those of the unPEGylated and targeted lipoplexes (Figure 3 *b*), as evidenced

by the integrity of the released pDNA bands on the gels. This reduction of pDNA protection by targeted lipoplexes is probably due to the effect of the negative charge of FA, which reduces the electrostatic interactions between the pDNA and cationic liposome, resulting in a slight decrease of pDNA condensation and protection. Duarte *et al.*<sup>23</sup> reported similar observations of reduction in pDNA protection by FA-conjugated lipoplexes, which was attributed to the reduction in pDNA compaction promoted by the presence of PEG in the lipoplexes. The effect of the negative charge of FA on lipoplex properties was also demonstrated by the lower zeta potential of FA-lipoplexes compared to that obtained for the corresponding non-targeted lipoplexes (Table 1), enforcing the notion that the slight decrease of pDNA condensation/protection induced by FA is related to the reduction of complex surface charge.

**EtBr dye displacement assay:** The degree of interaction of the cationic liposome with the pCMV-luc DNA as a function of liposome concentration was examined using an EtBr fluorescence quenching method. The displacement of fluorescence dye from DNA by cationic materials has been reported as an indicator of the complex-forming potential in DNA delivery systems<sup>24</sup>. As the  $\pm$  ratios increased, the relative fluorescence of the complexes decreased (increased complexation), regardless of liposome formulation, reaching a maximum binding degree and plateauing at  $\pm$  ratios of about 2 : 1 (Figure 3) for all preparations. The positive charge on the liposome allows binding of DNA through electrostatic interactions to form lipoplexes. The pDNA condensation capacity was seen to be the greatest for the unPEGylated-untargeted lipoplexes followed by the untargeted-PEGylated and targeted lipoplexes respectively. A similar result showing low DNA condensation in FA-targeted lipoplexes was reported elsewhere<sup>23</sup>, indicating that FA-liposomes do show higher EtBr accessibility to pDNA, which could be ascribed to a strong reduction in pDNA compaction promoted by PEG in the lipoplexes. The charge ratios ( $\pm$ ) at end-points found in this study for unPEGylated, PEGylated and targeted liposomes were 2 : 1, 2.4 : 1 and 2.6 : 1 respectively,

and are corroborative of those obtained in the retardation study (refer to Figure 2). Zhang *et al.*<sup>25</sup> suggested that PEGylation reduces the surface charge density of cationic liposomes and has a negative effect on nucleic acid binding affinities, which may result in weaker pDNA binding compared to plain liposomes.

*Size and zeta potential of the carrier system:* Size distribution and zeta potential of preparations were investigated by dynamic light scattering (DLS) (Table 1). Biophysical properties such as size, charge density and morphology of the resulting DNA complexes determine the transfection efficiencies of nonviral carriers<sup>26</sup>. Lipoplexes based on electrostatic interaction were prepared by self-assembly in HBS medium at room temperature. Size measurements (Table 1) demonstrated the suitability of liposome preparations for biomedical applications, as it indicated a size range 100–196 nm for both liposomes and lipoplexes, which are suitable for endocytotic cellular uptake. However, the unPEGylated lipoplex showed a marked increase in average size (695 nm). The large lipoplex size may have resulted from aggregation of lipoplexes at electroneutrality. The size of the lipoplex can decrease when its charge increases from the neutralization point. Non-viral vectors producing larger particle sizes with nucleic acids were reportedly effective at protecting DNA from attack by DNase I and increasing serum resistance<sup>27</sup>. It is also apparent that the particle sizes of preparations decreased after PEGylation (Table 1), a result that is consistent with the findings of other studies<sup>28</sup>. The size reduction seen in PEGylated lipoplexes is attributed to the packing effects of PEG chains into vesicle structures and steric repulsion<sup>29</sup>. UnPEGylated lipoplexes lacking the steric repulsion forces associated

with PEGylated liposomes and targeted PEGylated complexes were polydisperse (PDI = 0.57 and 0.47 respectively), while the untargeted PEGylated lipoplexes were of a more homogeneous size distribution (PDI = 0.21).

The zeta potential is a measure of the surface charge of colloidal dispersions. The zeta potential technique is generally employed to predict and control stability of colloidal dispersions. Electrostatic repulsion among the particles with identical electric charge prevents particle aggregation<sup>30</sup>. All liposome formulations showed positive zeta potential values (Table 1). In contrast, zeta potentials were lower for lipoplexes, as the liposome ionic charge is neutralized by the nucleic acid ionic charge at the time of complexation/interaction. On the other hand, a further drop in zeta potential from low positive to negative, is noticeable for both PEGylated, untargeted and targeted lipoplexes, which could be explained by the following: (a) low DNA condensation degree of PEGylated liposomes as indicated in gel retardation and EtBr intercalation assays, and (b) additional negative charge on folate contributing to the net negative zeta value for the folate targeted lipoplexes through the presence of  $\alpha$ -carboxyl groups in the molecular structure of the anchored ligand. In lipoplexes, incorporation of PEG into cationic liposomes resulted in the reduction of zeta potential. This reduction was greater when the PEGylation degree was higher, suggesting that PEGylation can perhaps reduce the surface charge density. Moreover, Li *et al.*<sup>31</sup> also suggested that F-CLs attained negative zeta potential values of  $-10$  and  $-12$ , at weight ratios 1 : 1 and 5 : 1 respectively.

#### Cytotoxicity evaluation of vector system

The toxic effect of MSO9 cationic liposomes to the cells was assessed through MTT assay. In this study, lipoplexes exhibited minimal toxicity which is highly desirable for gene delivery carriers. It is apparent that none of the lipoplexes had significant cytotoxicity at charge ratios selected for the study under the experimental conditions, as  $\sim 70\%$  cell viability was noted (Figure 5).

#### Gene transfection efficiency of lipoplexes

Generally, all three lipoplexes showed high gene transfection efficacy at  $\pm$  ratios tested, ranging from 1 : 1 to 4 : 1. The transfection patterns of MSO9 PEGylated lipoplexes for HeLa, KB, and HEK293 cells were somewhat similar to the MSO9 untargeted–unPEGylated lipoplexes (Figure 6a), except that the PEGylated lipoplex had higher transfection activities at  $\pm$  ratios 1 : 1, 2 : 1, and 3 : 1. Transfection activity of the PEGylated lipoplex was tenfold greater than that of the unPEGylated–untargeted lipoplexes. Interestingly, the level of reporter gene expression in all lipoplexes was consistently higher for the HeLa cells than for the KB and HEK293 cells,

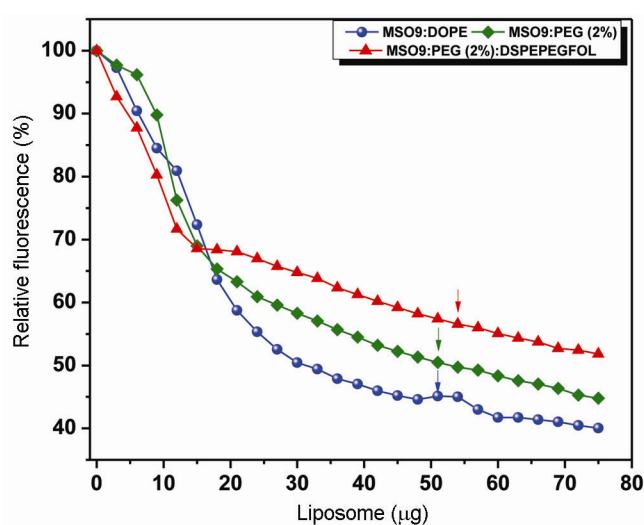


**Figure 4.** EtBr dye displacement assay. Reaction mixtures were incubated in a total volume of 100  $\mu$ l HBS. pCMV-luc DNA was kept constant at 1.2  $\mu$ g and liposome suspensions added systematically in 1  $\mu$ l aliquots.

because targeted reporter gene transfection activity depends, to a large extent, on the nature of the promoter, cell type and expression of cognate receptors<sup>32</sup>. FA-targeted lipoplexes resulted in a significant increase of luciferase gene expression in FR-positive cells. The luciferase expression levels were tenfold to one hundred fold higher than those attained with the other lipoplexes (Figure 6c). The inhibition of gene delivery by serum is considered to be one of the major limitations for lipoplex application *in vivo*.<sup>33</sup> With this in mind, transfection was investigated in the presence of serum. The elevated luciferase activity in FR-positive cells provided clear

evidence for their potential application *in vivo*. As reported in our previous work<sup>27</sup>, FA-targeted delivery can enhance the gene transfection for FR-positive cells in the presence of serum. These results confirm that the enhanced gene transfection accomplished by the receptor-mediated uptake approach in this study is likely to be due to the combined or synergistic effect of PEG and folate. In contrast, FR-negative HEK293 cells showed reduced transgene activity owing to the lack of FR-dependent endocytosis mechanism (Figure 6a-c).

Competition assays were carried out to validate that uptake of the MSO9 folate-labelled lipoplexes was a

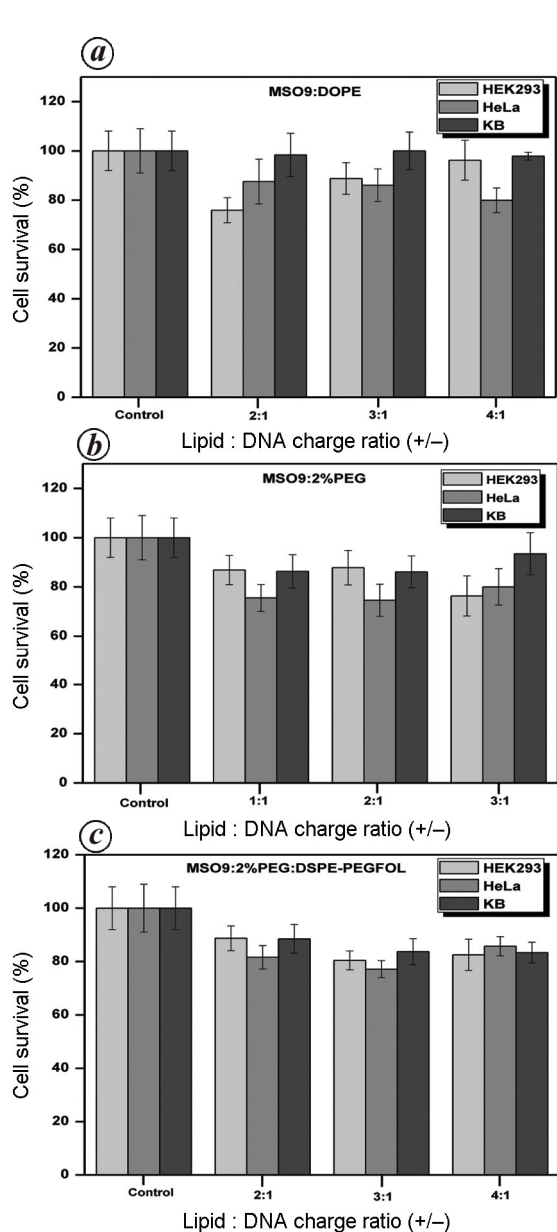


**Figure 5.** Cell viability assays of MSO9 lipoplexes containing 0.5  $\mu$ g pCMV-luc. a-c, Cell survival profiles of non-targeted lipoplexes (a), PEGylated lipoplexes (b), and targeted lipoplexes (c). Cells without liposome inclusion were used as control. Data represent the mean  $\pm$  SD of three wells.

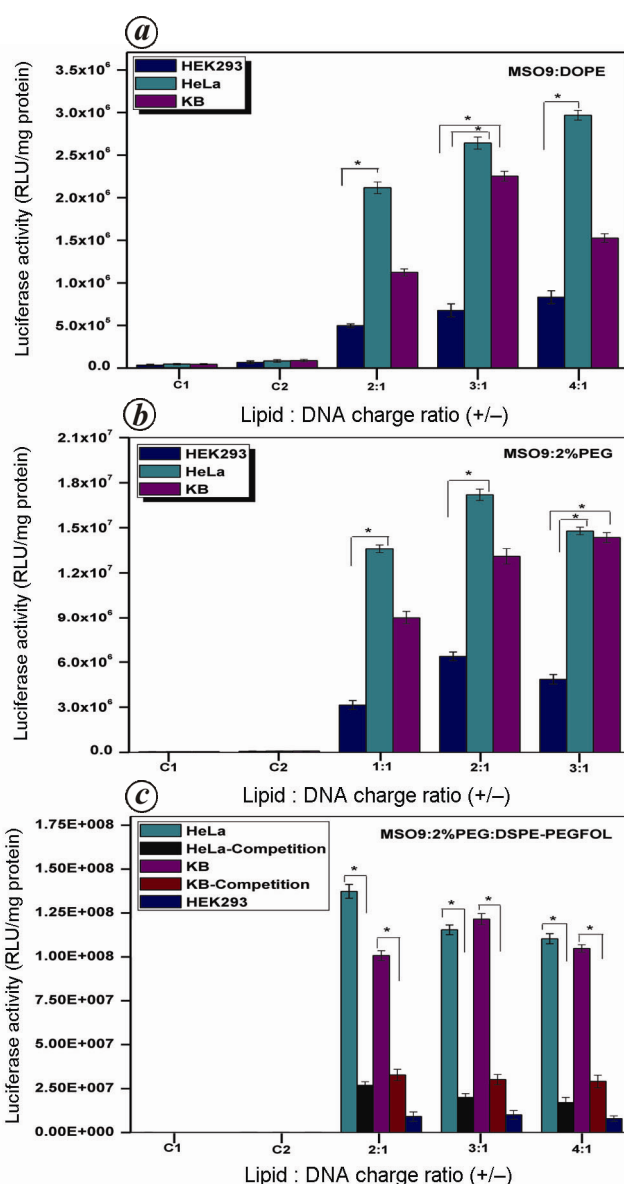


**Figure 6.** *In vitro* gene transfection efficiencies of MSO9 lipoplexes containing 0.5  $\mu$ g pCMV-luc. Gene expression profiles of non-targeted lipoplexes (a), PEGylated lipoplexes (b), and targeted lipoplexes (c). Control 1(1): Cells alone, Control 2(2): Cells with pDNA (0.5  $\mu$ g). For competition studies, 200  $\mu$ M folate was added prior to addition of targeted lipoplexes. Luciferase reporter gene activity is expressed as RLU/mg of protein. Data presented as mean  $\pm$  SD ( $n = 3$ ). \* $P < 0.05$ .

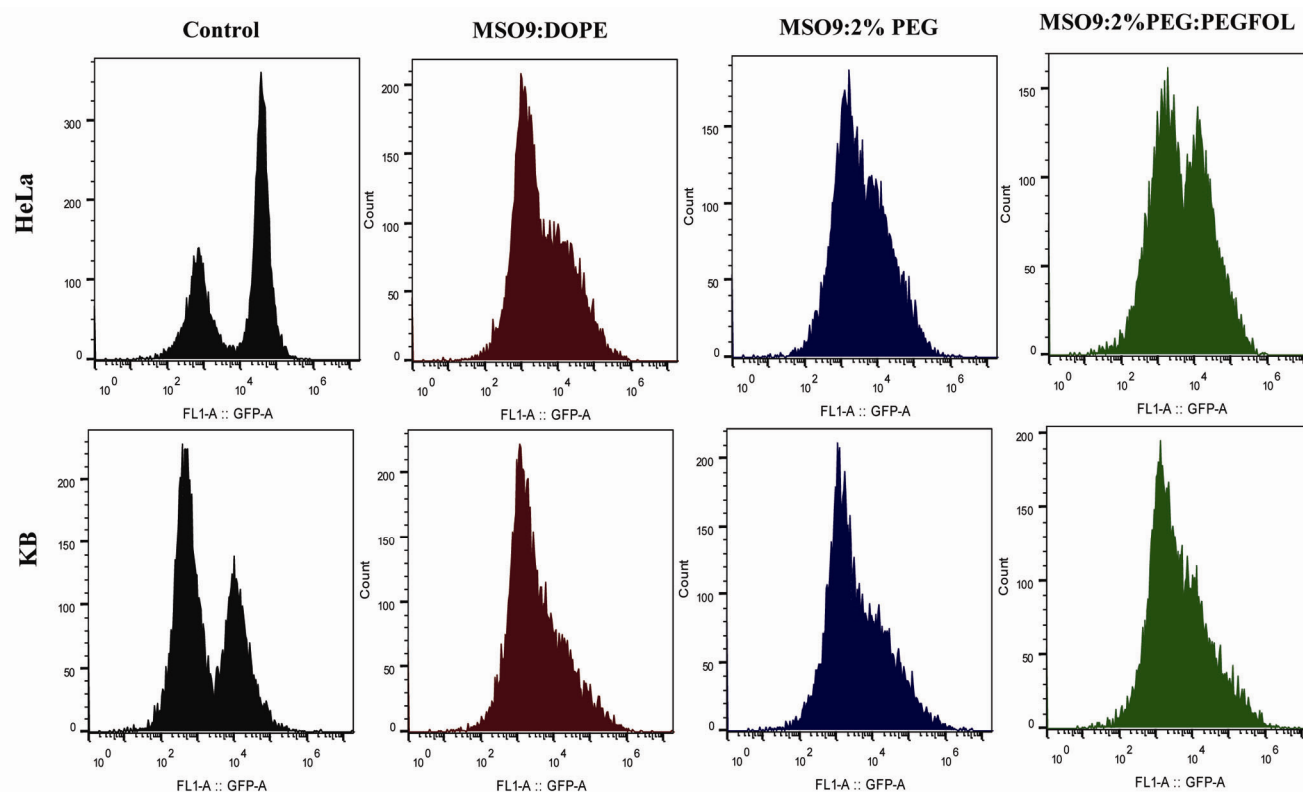


**Figure 7.** Flow cytometry showing the quantitative cellular uptake analysis of MSO9 complexes. Fluorescence intensities of untreated cells, untargeted, PEGylated and targeted MSO9 lipoplexes respectively in HeLa (upper row images) and KB (lower row images) cells. Results of the flow cytometry are shown in histograms with the x-axis indicating the mean fluorescence intensity and y-axis indicating cell count.

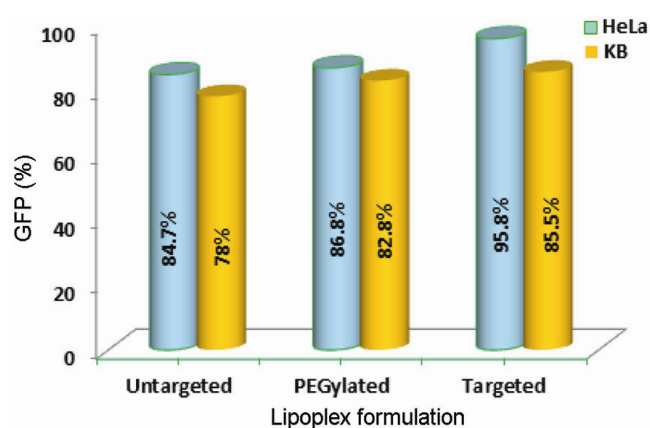


**Figure 8.** GFP fluorescence intensity of lipoplexes in HeLa and KB cells. Transfection of MSO9 untargeted, PEGylated and targeted lipoplexes respectively, at optimum ratios for transfection activity as confirmed in the luciferase assay.

target-cell-specific event. As shown in Figure 6c, the transfection activity of FA-labelled lipoplexes is significantly reduced when the FR-positive HeLa and KB cells are treated with excess FA. The results indicate that the folate ligand plays an important role in enhancing the transgene activity in FA-targeted lipoplexes by a receptor mediated endocytosis mechanism.

### Flow cytometry

Intracellular uptake of the transfecting lipoplexes was quantitatively studied using flow cytometry. Figure 7 represents GFP fluorescence intensity histograms of FR-positive HeLa and KB cells transfected with MSO9 untargeted, PEGylated and targeted lipoplexes along with that of the untreated cells as control. Results suggest that in general, the fluorescence intensity is higher in folate targeted lipoplexes than those of the untargeted lipoplexes (PEGylated or unPEGylated), which is in agreement with the luciferase transfection results.

The MSO9 lipoplexes showed moderate to strong fluorescence signals depending on the type of formulation. The order of mean fluorescence intensities observed in HeLa cells transfected with various MSO9 lipoplexes was as follows: PEGylated–targeted > PEGylated–untargeted > untargeted–unPEGylated lipoplexes with mean fluorescence intensity of 40354, 33172 and 32369 respectively. In KB cells, GFP mean fluorescence intensity noted for the MSO9 untargeted, PEGylated and targeted lipoplexes was 29258, 31056 and 32071 respectively. It is apparent from Figure 7 that cellular uptake of targeted lipoplexes is higher (broader fluorescence) compared to the untargeted lipoplexes both in HeLa and KB cells. This enforces the idea of the targeted lipoplex being receptor-dependent,

which is not the case for untargeted lipoplexes as they lack the receptor specificity. Tang *et al.*<sup>33</sup> noted the increased cell uptake efficiencies at increased FA densities on magnetic nanoparticles (MNPs) in HeLa cells, and postulated that it may be due to the FR-mediated internalization process. Thus, the result of this study demonstrates that the main internalization mechanism of the MSO9 targeted lipoplex is a FR-facilitated endocytosis pathway, specific to FR-overexpressing cells such as HeLa and KB cells. Figure 8 demonstrates the transfection efficiency of MSO9 lipoplexes in terms of percentage range. Enhanced cellular uptake can be deduced from the result for the MSO9 targeted lipoplexes compared to the untargeted, unPEGylated lipoplexes, which is in agreement with the flow cytometry histograms where the targeted lipoplexes exhibited broader fluorescence distributions.

## Conclusion

In this study, novel folate-labelled cationic liposomes were able to successfully and specifically target FR. The evaluated pharmaceutical parameters of these novel liposome carriers were favourable to gene delivery. These liposomes offered effective nucleic acid binding, cargo protection and possessed a narrow size distribution. Furthermore, transfection levels attained by the targeted MSO9 lipoplexes were higher in FR+ HeLa and KB cells than in FR-HEK293 cells. Luciferase activity attained by targeted lipoplexes was greatly reduced in the presence of excess folate in FR+ cells, confirming that the FA-targeted MSO9 lipoplexes were able to successfully target the FR+ cells and that the FR-dependent pathway was indeed the mode of cellular uptake of these targeted lipoplexes. In addition, the high levels of transgene expression in the presence of serum bodes well for future *in vivo* gene delivery applications. Further studies and optimizations are warranted to investigate the potential therapeutic advantage of these FR-targeted liposomal formulations for *in vivo* tumour targeting.

1. Tanaka, H., Akita, H., Ishiba, R., Tange, K., Arai, M., Kubo, K. and Harashima, H., Neutral biodegradable lipid-envelope-type nanoparticle using vitamin A-scaffold for nuclear targeting of plasmid DNA. *Biomaterials*, 2014, **35**, 1755–1761.
2. Tagalakis, A. D. *et al.*, PEGylation improves the receptor-mediated transfection efficiency of peptide-targeted, self-assembling, anionic nanocomplexes. *J. Control. Release*, 2014, **174**, 177–187.
3. Felgner, P. L. *et al.*, Lipofection: a highly efficient, lipid-mediated DNA-transfection procedure. *Proc. Natl. Acad. Sci. USA*, 1987, **84**, 7413–7417.
4. Parvizi, P. *et al.*, Aspects of nonviral gene therapy: correlation of molecular parameters with lipoplex structure and transfection efficacy in pyridinium-based cationic lipids. *Int. J. Pharm.*, 2014, **461**, 145–156.

5. Zheng, N. *et al.*, Maximizing gene delivery efficiencies of cationic helical polypeptides via balanced membrane penetration and cellular targeting. *Biomaterials*, 2014, **35**, 1302–1314.
6. Mintzer, M. A. and Simanek, E. E., Nonviral vectors for gene delivery. *Chem. Rev.*, 2009, **109**, 259–302.
7. Zuhorn, I. S., Engberts, J. B. F. N. and Hoekstra, D., Gene delivery by cationic lipid vectors: overcoming cellular barriers. *Eur. Biophys. J.*, 2007, **36**, 349–362.
8. Parvizi, P. *et al.*, Aspects of nonviral gene therapy: correlation of molecular parameters with lipoplex structure and transfection efficacy in pyridinium-based cationic lipids. *Int. J. Pharm.*, 2014, **461**, 145–156.
9. Yi, W.-J. *et al.*, Cyclen-based lipidic oligomers as potential gene delivery vehicles. *Acta Biomater.*, 2014, **10**, 1412–1422.
10. Huang, S. *et al.*, Tumor targeting and microenvironment-responsive nanoparticles for gene delivery. *Biomaterials*, 2013, **34**, 5294–5302.
11. Li, L., Yang, Q., Zhou, Z., Zhong, J. and Huang, Y., Doxorubicin-loaded, charge reversible, folate modified HPMA copolymer conjugates for active cancer cell targeting. *Biomaterials*, 2014, **35**, 5171–5187.
12. Guo, Z. *et al.*, Targeting efficiency of RGD-modified nanocarriers with different ligand intervals in response to integrin  $\alpha v \beta 3$  clustering. *Biomaterials*, 2014, **35**, 6106–6117.
13. Zhao, J. and Feng, S. S., Effects of PEG tethering chain length of vitamin E TPGS with a herceptin-functionalized nanoparticle formulation for targeted delivery of anticancer drugs. *Biomaterials*, 2014, **35**, 3340–3347.
14. Gao, W., Xiang, B., Meng, T.-T., Liu, F. and Qi, X.-R., Chemotherapeutic drug delivery to cancer cells using a combination of folate targeting and tumor microenvironment-sensitive polypeptides. *Biomaterials*, 2013, **34**, 4137–4149.
15. Valencia, P. M., Hanewich-Hollatz, M. H., Gao, W., Karim, F., Langer, R., Karnik, R. and Farokhzad, O. C., Effects of ligands with different water solubilities on self-assembly and properties of targeted nanoparticles. *Biomaterials*, 2011, **32**, 6226–6233.
16. Wang, X. *et al.*, The development of site-specific drug delivery nanocarriers based on receptor mediation. *J. Control. Release*, 2014, **193**, 139–153.
17. Hattori, Y., Kubo, H., Higashiyama, K. and Maitani, Y., Folate-linked nanoparticles formed with DNA complexes in sodium chloride solution enhance transfection efficiency. *J. Biomed. Nanotechnol.*, 2005, **1**, 176–184.
18. Singh, M. and Ariatti, M., A cationic cytofectin with long spacer mediates favourable transfection in transformed human epithelial cells. *Int. J. Pharm.*, 2006, **309**, 189–198.
19. *Control Release Soc. Newsl.*, 2013, **30**, 1568–1579; [www.controlledreleasesociety.org](http://www.controlledreleasesociety.org).
20. Choi, J. S., Nam, K., Park, J., Kim, K. B. and Lee, J. K., Enhanced transfection efficiency of PAMAM dendrimer by surface modification with L-arginine. *J. Control. Release*, 2004, **99**, 445–456.
21. Sheng, R., Luo, T., Li, H., Sun, J., Wang, Z. and Cao, A., Cholesterol-based cationic lipids for gene delivery: contribution of molecular structure factors to physicochemical and biological properties. *Colloids Surf. B*, 2014, **116**, 32–40.
22. Hatakeyama, H. *et al.*, Systemic delivery of siRNA to tumors using a lipid nanoparticle containing a tumor-specific cleavable PEG-lipid. *Biomaterials*, 2011, **32**, 4306–4316.
23. Duarte, S., Faneca, H. and Pedrosa de Lima, M. C., Non-covalent association of folate to lipoplexes: a promising strategy to improve gene delivery in the presence of serum. *J. Control. Release*, 2011, **149**, 264–272.
24. Tang, M. X. and Szoka, F. C., The influence of polymer structure on the interactions of cationic polymers with DNA and morphology of the resulting complexes. *Gene Therapy*, 1997, **4**, 823–832.



## RESEARCH ARTICLES

---

25. Zhang, Y. *et al.*, DC-Chol/DOPE cationic liposomes: a comparative study of the influence factors on plasmid pDNA and siRNA gene delivery. *Int. J. Pharm.*, 2010, **390**, 198–207.
26. Esposito, C., Generosi, J., Mossa, G., Masotti, A. and Castellano, A. C., The analysis of serum effects on structure, size and toxicity of DDAB–DOPE and DC–Chol–DOPE lipoplexes contributes to explain their different transfection efficiency. *Colloids Surf. B*, 2006, **53**, 187–192.
27. Almofti, M. R., Harashima, H., Shinohara, Y., Almofti, A., Li, M. and Kiwada, H., Lipoplex size determines lipofection efficiency with or without serum. *Mol. Membr. Biol.*, 2003, **20**, 35–43.
28. Kim, H.-K., Dava, E., Myung, C.-S. and Park, J.-S., Enhanced siRNA delivery using cationic liposomes with new polyarginine-conjugated PEG-lipid. *Int. J. Pharm.*, 2010, **392**, 141–147.
29. Maitani, Y., Nakamura, A., Tanaka, T. and Aso, Y., Hydration of surfactant-modified and PEGylated cationic cholesterol-based liposomes and corresponding lipoplexes by monitoring a fluorescent probe and the dielectric relaxation time. *Int. J. Pharm.*, 2012, **427**, 372–378.
30. Wei, K., Peng, X. and Zou, F., Folate-decorated PEG–PLGA nanoparticles with silica shells for capecitabine controlled and targeted delivery. *Int. J. Pharm.*, 2014, **464**, 225–233.
31. Li, H. *et al.*, Delivery of calf thymus DNA to tumor by folate receptor targeted cationic liposomes. *Biomaterials*, 2011, **32**, 6614–6620.
32. Boussif, O., Lezoualcht, F., Zanta, M. A., Mergny, M. D., Schermant, D., Demeneix, B. and Behr, J.-P., A versatile vector for gene and oligonucleotide transfer into cells in culture and *in vivo*: polyethylenimine. *Proc. Natl. Acad. Sci., USA*, 1995, **92**, 7297–7301.
33. Tang, Z., Li, D., Sun, H., Guo, X., Chen, Y. and Zhou, S., Quantitative control of active targeting of nanocarriers to tumor cells through optimization of folate ligand density. *Biomaterials*, 2014, **35**, 8015–8027.

ACKNOWLEDGEMENTS. We thank the National Research Foundation (68339, 88195) and the College of Agriculture, Engineering and Science, School of Life Sciences, University of KwaZulu-Natal, Westville Campus, Durban, South Africa for funds.

Received 2 July 2015; revised accepted 29 February 2016

doi: 10.18520/cs/v111/i4/662-670

---